MOLECULAR AND CELLULAR BIOLOGY, Jan. 2004, p. 638–650 Vol. 24, No. 2
0270-7306/04/$08.00+0 DOI: 10.1128/MCB.24.2.638–650.2004

EMILIN-1 Deficiency Induces Elastogenesis and Vascular Cell Defects

Miriam Zanetti,[1]† Paola Braghetta,[1]† Patrizia Sabatelli,[2] Isabella Mura,[3] Roberto Doliana,[4] Alfonso Colombatti,[4] Dino Volpin,[1] Paolo Bonaldo,[1] and Giorgio M. Bressan[1]*

Department of Histology Microbiology and Medical Biotechnologies, University of Padua, 35100 Padua,[1] Istituto per i Trapianti d'Organo e l'Immunocitologia, CNR,[2] and Unità Neuromuscolare, Istituti Ortopedici Rizzoli,[3] 40136 Bologna, and Divisione di Oncologia Sperimentale, CRO-IRCCS, 33081 Aviano,[4] Italy

Received 26 March 2003/Returned for modification 28 May 2003/Accepted 8 October 2003

EMILINs constitute a family of genes of the extracellular matrix with high structural similarity. Four genes have been identified so far in human and mouse. To gain insight into the function of this gene family, EMILIN-1 has been inactivated in the mouse by gene targeting. The homozygous animals were fertile and did not show obvious abnormalities. However, histological and ultrastructural examination revealed alterations of elastic fibers in aorta and skin. Formation of elastic fibers by mutant embryonic fibroblasts in culture was also abnormal. Additional alterations were observed in cell morphology and anchorage of endothelial and smooth muscle cells to elastic lamellae. Considering that EMILIN-1 is adhesive for cells and that the protein binds to elastin and fibulin-5, EMILIN-1 may regulate elastogenesis and vascular cell maintenance by stabilizing molecular interactions between elastic fiber components and by endowing elastic fibers with specific cell adhesion properties.

EMILINs are a family of proteins of the extracellular matrix that are characterized by a unique arrangement of structural domains, including a signal peptide and the EMI domain, a cysteine-rich sequence of about 80 amino acids, at the amino terminus; an alpha-helical domain with high probability for coiled-coil structure formation in the central part of the molecule; and a region homologous to the globular domain of C1q (gC1q domain) at the carboxyl-terminal end (10, 18). High sequence similarity between EMILINs is found in the EMI and gC1q domains. Amino acid similarity is low in the coiled-coil region; however, the structural feature of the heptad repeat, which is necessary for coiled-coil structure formation, is conserved. The first protein of the family, initially named gp115, was isolated from chicken aorta under harsh solubilizing conditions and found to be particularly abundant in that tissue (4). Immunohistochemistry studies confirmed that the protein was strongly expressed in blood vessels, and, in addition, they revealed its presence in connective tissues of a wide variety of organs (9), particularly in association with elastic fibers (11). At the ultrastructural level, the molecule was detected in elastic fibers, where it was located at the interface between the amorphous core and the surrounding microfibrils (5). On the basis of this finding, the protein was named EMILIN (elastin microfibril interface-located protein). Cloning of the cDNA of chicken EMILIN has brought about the isolation of the human and mouse genes (17, 18). The extensive sequence information available for these species in databases has allowed the identification of three other homologous molecules, thus defining a new gene family. The family includes, in addition to the protein first isolated and now renamed EMILIN-1, a closely related molecule, EMILIN-2 (16); multimerin, a protein secreted by endothelial cells and platelets (19); and endoglyx-1, a pan-endothelial human cell surface glycoprotein (6). The latter two molecules, also known as EMILIN-3 and multimerin-2, respectively (15, 24), share high homology to each other and have similar gene organizations.

At present the function of any EMILIN is unknown. The finding that antibodies against EMILIN-1 inhibited elastin deposition by smooth muscle cells in vitro suggests that the protein may play a role in elastogenesis (5). Accordingly, biosynthetic and immunodetection studies have shown that elastin-producing cells, such as smooth muscle cells, fibroblasts, and endothelial cells, are major sources of EMILIN-1 synthesis and deposition into the extracellular matrix (5, 8). On the other hand, the detection of EMILIN-1 mRNA in ectoplacental cone, trophoblast giant cells, extraembryonic ectoderm, and extraembryonic visceral endoderm of developing mouse embryos favors the idea of additional functions (3). This is also indicated by the observation that EMILIN-1 has adhesive properties for different types of cells (18, 32).

To gain insight into the function of EMILINs, we have generated mice disrupted at the EMILIN-1 gene locus. The homozygous animals are fertile, have a normal life span, and do not exhibit gross morphological abnormalities. A closer examination, however, shows alterations of the fine structure of elastic fibers and of cell morphology in elastic arteries. We also find that EMILIN-1 binds elastin and fibulin-5 and that association of fibulin-5 with elastin is altered in the absence of EMILIN-1. These interactions explain the localization of EMILIN-1 between the amorphous core and microfibrils and suggest that the protein may stabilize elastic fibers through defined molecular interactions and influence cell behavior by contributing specific cell adhesion properties to elastic fibers.

* Corresponding author. Mailing address: Dipartimento di Istologia Microbiologia e Biotecnologie Mediche, Università di Padova, Viale G. Colombo, 3, 35121 Padua, Italy. Phone: 390498276086. Fax: 390498276079. E-mail: bressan@civ.bio.unipd.it.

† M.Z. and P.B. contributed equally to this work.

MATERIALS AND METHODS

Construction of the targeting vector. A 135-kb BAC clone containing the murine EMILIN-1 locus was isolated from a 129/SvJ genomic library (Genome Systems, Inc.) by screening with a murine EMILIN-1 cDNA fragment, and the exon-intron organization was determined (17). A 5.6-kb *Xba*I-*Kpn*I fragment containing the 5′ flanking region, the first exon, and part of the first intron of the EMILIN-1 gene was used for the construction of the targeting vector (Fig. 1A). A *lacZ-pgk-neo* cassette (21), containing the neomycin resistance gene under the control of the phosphoglycerol kinase promoter and poly(A) signal, was inserted in forward orientation into an *Xho*I site in the first exon. The targeting vector contained 4.8 kb of homology in the 5′ arm and 0.8 kb of homology in the 3′ arm. A thymidine kinase (*tk*) cassette was ligated at the 5′ end of the construct for negative selection. The *neo* cassette interrupts the coding sequence of EMILIN-1 at amino acid 27, leaving only the signal peptide and the first 6 amino acids of the mature protein.

Generation of EMILIN-1-deficient mice. A total of 6×10^7 R1 embryonic stem (ES) cells (28) were electroporated with 250 μg of *Not*I-linearized targeting vector and selected as previously described (2). Five positive recombinant clones were identified and checked for correct single integration by Southern blot analysis. Two correctly targeted ES cell clones (ES-34 and ES-289) were used to generate germ line chimeric mice by injection into C57BL/6 host blastocysts (20). The resulting male chimeras were bred to C57BL/6 or CD1 females, to obtain heterozygous (Emi1$^{+/-}$) F_1 mice, which were intercrossed to produce homozygous null (Emi1$^{-/-}$) mice. Homozygous mice obtained from the two independent ES cell clones were used for all the subsequent analysis.

Genotype analysis. Genomic DNA was isolated from ES cells, embryos, or tail biopsies as described previously (23), digested with *Dra*I, separated on 0.8% agarose gels, transferred to a Gene Screen membrane (Dupont), and hybridized with a 1.0-kb *Bam*HI-*Eco*RI genomic fragment as an external probe (Fig. 1A). Insertion of the *neo* cassette introduced a *Dra*I site that could be used to distinguish the wild-type and the targeted alleles, which produced 5.2- and 2.8-kb fragments, respectively. The membranes were rehybridized with *neo* and *tk* probes to verify that a correct single integration had occurred.

Cell cultures and transfections. Primary fibroblasts were isolated as described previously (20) from the carcasses of embryos at 13.5 days postcoitum obtained by Emi1$^{+/-}$ $F_1 \times F_1$ intercrosses, and cultured in Dulbecco's minimal essential medium (DMEM) supplemented with 10% fetal calf serum (FCS). For immunofluorescence, the cells were plated into gelatinized Permanox chamber slides (Nunc) (10,000 to 20,000 cells/well) and grown for 9 to 15 days. 293T cells were propagated in the same culture medium (DMEM plus 10% FCS) and transfected by the calcium phosphate procedure (1) at a density of 2.2×10^6 cells/10-cm-diameter petri dish. Before harvesting, the cells were incubated in 1.5 ml of DMEM without FCS for 2 days.

Northern blotting and reverse transcriptase PCR (RT-PCR) analysis. RNA was extracted from normal and mutant embryos or tissues by using TRIzol reagent (Gibco-BRL). For Northern blot analysis, 15 μg of total RNA were separated in 1% agarose–formaldehyde gels, blotted onto Hybond-N membranes (Amersham), and hybridized with a 1.2-kb fragment spanning the 3′ region of murine EMILIN-1 cDNA (3) and a cDNA fragment for human glyceraldehyde-3-phosphate dehydrogenase (GAPDH) as loading control (33).

RT-PCR analysis was performed as follows. First-strand cDNA was synthesized from 1 μg of total RNA by using Superscript reverse transcriptase (Gibco-BRL) and random hexamers as specified by the manufacturer. PCR was then carried out for 25 to 45 cycles with the following specific primer sets: (i) EMILIN-1, 5′-CCAGCACCCTCCACACCACTTC-3′ and 5′-AGCTGCTGCAACT TCTCTGACTC-3′, producing a fragment of 128 bp, and (ii) eucaryotic translation initiation factor 1A (eIF1A), 5′-AAGAAGTCTGAAGGCCTATG-3′ and 5′-CAGAGAACTTGGAATGTAGC-3′, giving rise to a fragment of 180 bp.

Immunofluorescence. Tissues from 15-day-old wild-type and mutant mice were frozen in liquid nitrogen, and 8- to 10-μm sections were collected on positively charged slides (BDH Superfrost Plus). Embryonic fibroblasts grown in chamber slides (Nunc) were washed twice with phosphate-buffered saline (PBS) and air dried. Both tissue sections and fibroblasts were fixed in either cold methanol or 4% paraformaldehyde in PBS for 2 to 5 min before processing. Primary and secondary antibodies were diluted in 5% goat serum. The antibodies used were the following: polyclonal rat serum against mouse recombinant EMILIN-1 (dilution, 1:6,400); polyclonal rabbit serum against mouse recombinant tropoelastin fragments, a gift from R. Mecham or purchased from Elastin Products Company Inc. (dilution, 1:50); rabbit antiserum against fibulin-2, a gift from R. Timpl (dilution, 1:200); rabbit antiserum against fibulin-5, a gift from H. Yanagisawa (dilution, 1:200); mouse monoclonal antibody against human fibronectin, produced by hybridoma HB91 supplied by the American Type Culture Collection (undiluted supernatant); goat anti-rat Cy3-conjugated antibody, from Jackson Immuno Research (dilution, 1:400); goat anti-rabbit Cy2-conjugated antibody, from Jackson Immuno Research (dilution, 1:200); and goat anti-mouse tetramethyl rhodamine isocyanate-conjugated antibody, from Sigma (dilution, 1:200). Slides were incubated for 2 h at room temperature or overnight at 4°C with the primary antibody. After washing in PBS, secondary antibody was applied for 1 h at room temperature. The slides were mounted in 80% glycerol in PBS and observed in a Zeiss Axioplan microscope equipped with epifluorescence optics or in a Bio-Rad confocal microscope.

For elastin–fibulin-5 or elastin–fibrillin-1 double immunofluorescence, in which two rabbit antisera had to be used, immunoglobulins from the polyclonal antiserum against mouse elastin were purified by protein A (Amersham) affinity chromatography and labeled with Alexa Fluor 568 (Molecular Probes) as described by the manufacturer. A ratio of 5.2 mol of fluorochrome per mol of antibody was obtained. The immunoglobulins were used to label samples that had been completely processed through the indirect immunofluorescence procedure with anti-fibulin-2, -fibulin-5, or -fibrillin-1 antisera. The incubation conditions were similar to those described for primary antibodies (see above).

Histology. Tissue specimens were fixed overnight in 4% paraformaldehyde, dehydrated in a graded series of ethanol-water mixtures, and embedded in paraffin. Sections (7 μm) were stained by the Weigert resorcin-fuchsin method. Semithin sections (1 μm) obtained from Epon-embedded samples (see "Electron microscopy" below) were similarly stained.

Electron microscopy. Aortas and skin fragments were dissected from 15-day-old and adult wild-type and mutant mice, fixed with 2.5% glutaraldehyde in 0.1 M sodium cacodylate buffer (pH 7.4) overnight, washed in 0.1 M sodium cacodylate buffer overnight, and treated with 2% tannic acid in 0.1 M sodium cacodylate buffer as previously described (14). All samples were dehydrated with ethanol and embedded in Epon E812. Ultrathin sections were obtained from several blocks, stained with lead citrate and uranyl acetate, and observed in a Philips EM 400 transmission electron microscope operated at 100 kV. Sections obtained from aorta blocks were observed at the same magnification (×30,000).

Protein interaction studies. For solid-phase binding assays, recombinant aggregated EMILIN-1 was produced as described previously (27). Monomeric EMILIN-1, in which each molecule is formed by three identical polypetide chains (27), was obtained by reduction of the aggregated form (160 μg/ml) with 2.5 mM dithioerithritol for 1 h at 30°C and alkylation by addition of 5 mM iodoacetamide. Chicken α-elastin was produced from 7-day-old aortas (30). Vitronectin was purified from human plasma as described previously (35). A laminin-1/10/11 complex was purified from adult bovine kidney according to published procedures (25). Type VI collagen was purified from human placenta as described previously (7). Human lung α-elastin was purchased from Elastin Products Company, Engelbreth-Holm-Swarm laminin was from Sigma, type I collagen was from Collagen Corporation, and fibronectin was from Calbiochem-Novabiochem Corporation. For the assay, 10 μg of protein per ml was diluted in 0.1 M carbonate buffer (pH 9.6), and 0.5 to 1.0 μg/well was plated onto 96-well plates (Greiner) for 16 h at 4°C. After three washes with PBS, the nonspecific binding sites were blocked with 2% (wt/vol) bovine serum albumin (BSA) in PBS for 2 h at 4°C. The coated wells were then incubated with serial dilutions of the ligand for 60 min at room temperature, washed three times, and incubated with affinity-purified rabbit antibodies against EMILIN-1 (27) or rabbit antiserum against human α-elastin (TP 592; Elastin Products Company) or against chicken α-elastin (12) for 1 h. After three washes, the wells were incubated with horseradish peroxidase (HRP)-conjugated rabbit immunoglobulins for 1 h and washed again. Bound ligands were detected by a color reaction for 3 to 5 min with the addition of 2,2′-azino-bis(3-ethylbenz-thiazoline-6-sulfonic acid) and 0.01% H_2O_2. Color yields were determined as optical density at 405 nm. The amounts of ligands and antibody dilutions used were determined in preliminary experiments to give optimal color development. Specific binding was determined by subtracting the background binding of antibodies to immobilized proteins.

For immunoprecipitation experiments, 293T cells were transfected with 15 μg of a 1:1 mixture of pEMILIN, containing the entire cDNA coding sequence of human EMILIN-1 (27), and pElastin, including the complete cDNA of human elastin obtained by RT-PCR amplification and ligation of fragments of the coding sequence in vector pCEPy, a variant of pCEPu (22). The serum-free conditioned medium (see above) was supplemented with a mixture of protease inhibitors (Complete, Mini, and EDTA-free; Roche) and one-fifth of the volume of 5× lysis buffer (50 mM Tris [pH 7.5], 150 mM NaCl, 2 mM EDTA, 0.1% NP-40) containing 10% glycerol and kept on ice. The cell layer was taken up in 1 ml of lysis buffer containing protease inhibitors, 0.5% BSA, and 10% glycerol; frozen at −80°C; thawed; and centrifuged to remove cell debris. A similar procedure was used when 293T cells were transfected with a mixture of pElastin and pcDNA5/FRT/fibulin-5-V5-His, including rat fibulin-5 cDNA (34); the only

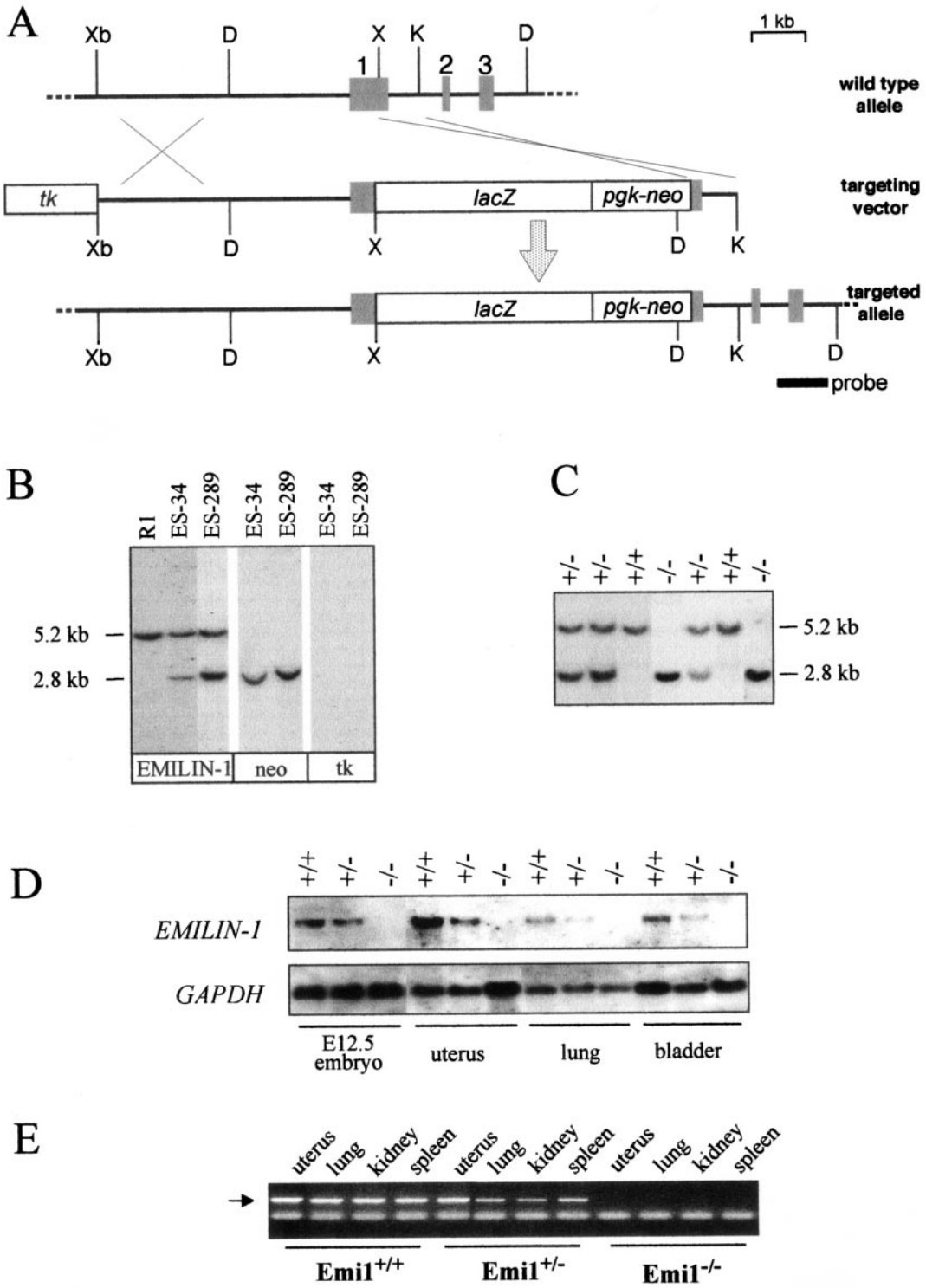

FIG. 1. Generation of EMILIN-1-deficient mice. (A) Strategy of EMILIN-1 locus targeting and probes used for Southern blotting and PCR analysis. Restriction sites: D, *Dra*I; K, *Kpn*I; X, *Xho*I; Xb, *Xba*I. (B) Characterization of targeted ES cell clones by Southern blotting. Hybridization of *Dra*I-digested DNA with an external probe reveals the expected fragments for the normal allele (5.2 kb) and the mutated allele (2.8 kb). Hybridization with the *neo* probe shows a single insertion of the cassette at the correct size. No signal is obtained with the *tk* probe, indicating that the *tk* cassette was lost during homologous recombination. (C) Distribution of genotypes of one $F_1 \times F_1$ litter. (D) Absence of mRNA for EMILIN-1 in whole embryos and adult tissues from Emi1$^{-/-}$ mice revealed by Northern blotting. E12.5, embryonic age 12.5 days postcoitum. (E) Absence of mRNA for EMILIN-1 in a set of adult tissues from Emi1$^{-/-}$ mice revealed by RT-PCR.

TABLE 1. Genotypes of progeny from Emi1$^{+/-}$ intercrosses[a]

ES cell clone	Mouse strain	No. of animals	No. (%) with genotype:		
			+/+	+/−	−/−
34	CD1	104	28 (27)	50 (48)	12 (25)
	C57/BL6	88	28 (32)	42 (48)	13 (20)
289	CD1	65	17 (26)	31 (48)	17 (26)
	C57/BL6	214	63 (29)	103 (48)	48 (23)
Total	CD1	169	45 (27)	81 (48)	43 (25)
	C57/BL6	302	91 (30)	145 (48)	66 (22)

[a] F_1 animals were used.

difference was the omission of EDTA and the addition of 1 mM $CaCl_2$ and 1 mM $MgCl_2$ in lysis buffer. For immunoprecipitation, 2.5 μl of antiserum (anti-human α-elastin or anti-fibulin-5) was added to 500-μl aliquots of conditioned medium or cell extract and the samples were incubated overnight at 4°C under agitation. After addition of 30 μl of protein A-agarose equilibrated in wash buffer (50 mM Tris [pH 7.5], 150 mM NaCl, 0.1% BSA, 0.1% NP-40, and 10% glycerol with or without $CaCl_2$-$MgCl_2$ and EDTA as described for the lysis buffer), the samples were incubated for 2 h at 4°C with agitation, centrifuged at 500 × *g* for 5 min, washed three times for 10 min each with wash buffer in which the NP-40 concentration had been increased to 0.5%, resuspended in 30 μl of Laemmli final sample buffer, boiled for 5 min in the presence of 5% beta-mercaptoethanol, and centrifuged, and the supernatant was resolved by sodium dodecyl sulfate-polyacrylamide gel electrophoresis (SDS-PAGE) (1). Protein-protein interaction was revealed by Western blotting with the SuperSignal West Pico Trial kit (Pierce) and the antibody against human EMILIN-1 diluted 1:1,000.

Detection of elastin polypeptides in aorta extracts. Pooled aortas obtained from 5- to 7-day-old wild-type and EMILIN-1-deficient mice were washed in PBS, minced, and extracted for 2 h in 40 mM Tris-HCl (pH 7.5) containing 8 M urea,1 mM EDTA, and protease inhibitors. The insoluble material was removed by centrifugation at 20,000 × *g*, and the protein content in the supernatant was determined with the Bio-Rad protein assay. Tissue extracts of equivalent protein content were analyzed by SDS-PAGE under reducing and nonreducing conditions with 4 to 20% Criterion gradient gels (Bio-Rad). For immunoblotting, resolved proteins were electrotransferred onto nitrocellulose membranes, which were subsequently saturated with PBS containing 1% α-casein for 2 h at room temperature and incubated with primary antibodies (either anti-chicken α-elastin diluted 1:5,000, anti-human α-elastin diluted 1:4,000, or antiserum to mouse recombinant tropoelastin fragments diluted 1:1,000, with similar results) at 4°C overnight. After extensive washing in PBS–0.1% α-casein, the membranes were incubated with HRP-conjugated goat anti-rabbit antibodies and then revealed with the ECL Plus chemiluminescence kit (Amersham Pharmacia Biotech, Cologno Monzese, Italy). Normalization of protein loading was further evaluated by immunoblotting with antibody against α-tubulin (Sigma).

RESULTS

The EMILIN-1 gene was inactivated by insertion of the *lacZ-pgk-neo* cassette into exon 1 (Fig. 1A). This truncates the coding sequence at amino acid 27, just after the signal peptide, and consequently no functional domains of EMILIN-1 should be contained in the translation product of the mutated gene. Two independent homologous recombinant ES cell clones were selected by Southern blotting (Fig. 1B), and the results obtained with each of them were identical (see below). Litters generated by Emi1$^{+/-}$ intercrosses exhibited a Mendelian distribution of genotypes in two different genetic backgrounds (Table 1 and Fig. 1C). Hetero- and homozygous mutant animals were fertile, had growth rates indistinguishable from that of controls, and did not show any gross abnormality.

Different experiments showed that expression of EMILIN-1 was completely abolished in homozygous mutants. EMILIN-1 mRNA was assayed in whole embryos and in different organs of adult animals by Northern blotting and RT-PCR; the mRNA was undetectable in Emi1$^{-/-}$ animals, while half of the normal amount was found in Emi1$^{+/-}$ mice (Fig. 1D and E). Moreover, tissue sections from adult animals were analyzed by immunofluorescence with a specific antibody against EMILIN-1 (Fig. 2). A network of short and fine fibrils was present in connective tissues of control mice (Fig. 2A and C) but was completely absent in sections prepared from homozygous mutants (Fig. 2B and D). Finally, fibroblasts were isolated from embryos at 13.5 days postcoitum and cultures stained by immunofluorescence with the EMILIN-1 antibody. As shown in Fig. 3A, normal cells deposited a meshwork rich in EMILIN-1 fibrils in the extracellular matrix. This meshwork was totally lacking in cultures of fibroblasts derived from Emi1$^{-/-}$ embryos (Fig. 3B). In contrast, the accumulation of fibronectin fibrils was similar in both types of cultures (Fig. 3C and D).

Histological analysis of different tissues and organs of Emi1$^{-/-}$ mice, including heart, lung, intestine, uterus, cornea, sclera, vibrissae, and skin, where EMILIN-1 is highly expressed during development (3), did not reveal any clear abnormality. The only exception was aorta after Weigert staining, a method specific for elastin. Subtle but consistent alterations included a very irregular outline, recurrent delamination, and increased interruption of elastic lamellae, more clearly seen in cross-sections (Fig. 4A and B), and a dishomogeneous and frayed texture of lamellae and accumulation of small elastin deposits between the lamellae seen in oblique or tangential sections (Fig. 4C and D). Moreover, regions of fragmentation of elastic lamellae, which were never seen in control samples, could be seen in semithin sections (Fig. 4E and F).

In the electron microscope, differences between normal and EMILIN-1-deficient elastic fibers could be found not only in aorta but also in the skin. The basic anomaly was similar in both tissues: the surface of the amorphous core was not smooth, as it was in control specimens, but was irregular, giving to the fiber a porous appearance; the coat of microfibrils, in contrast, was normal looking (Fig. 5A and B). Electron microscopy also disclosed important alterations of cells, specifically in aorta. The frequency of these alterations was highly significant, as revealed by statistical comparison of aorta cells from substantial numbers of control and EMILIN-1-deficient mice (Table 2). A recurrent finding was the increased space between the endothelial cell membrane and the internal elastic lamella (Fig. 5C and D); in normal aorta these structures were closely juxtaposed to each other and the enclosed narrow space was tightly packed with parallel fibrils, while it was enlarged and loosely filled with fibrillar material with random orientation in EMILIN-1-deficient tissue. At sites of interruption of the internal elastic lamella the gap was particularly wide and was crossed by endothelial cell protrusions (Fig. 5E). Abnormal cell surface-elastic fiber connections were also observed for smooth muscle cells. In normal aorta, elastin extensions radiated from elastic lamellae in a regular pattern and terminated on the plasma membrane at a cytoplasmic condensation (Fig. 5F). In knockout animals, this junctional setup was often disarranged, and cells appeared to have lost their firm adhesion to elastin (Fig. 5G and H). Abnormal cells exhibited an enlarged endoplasmic reticulum, swollen or dense mitochondria, and, more rarely, nuclei with condensed chromatin or pycnotic. Similar traits were also noted in endothelial cells

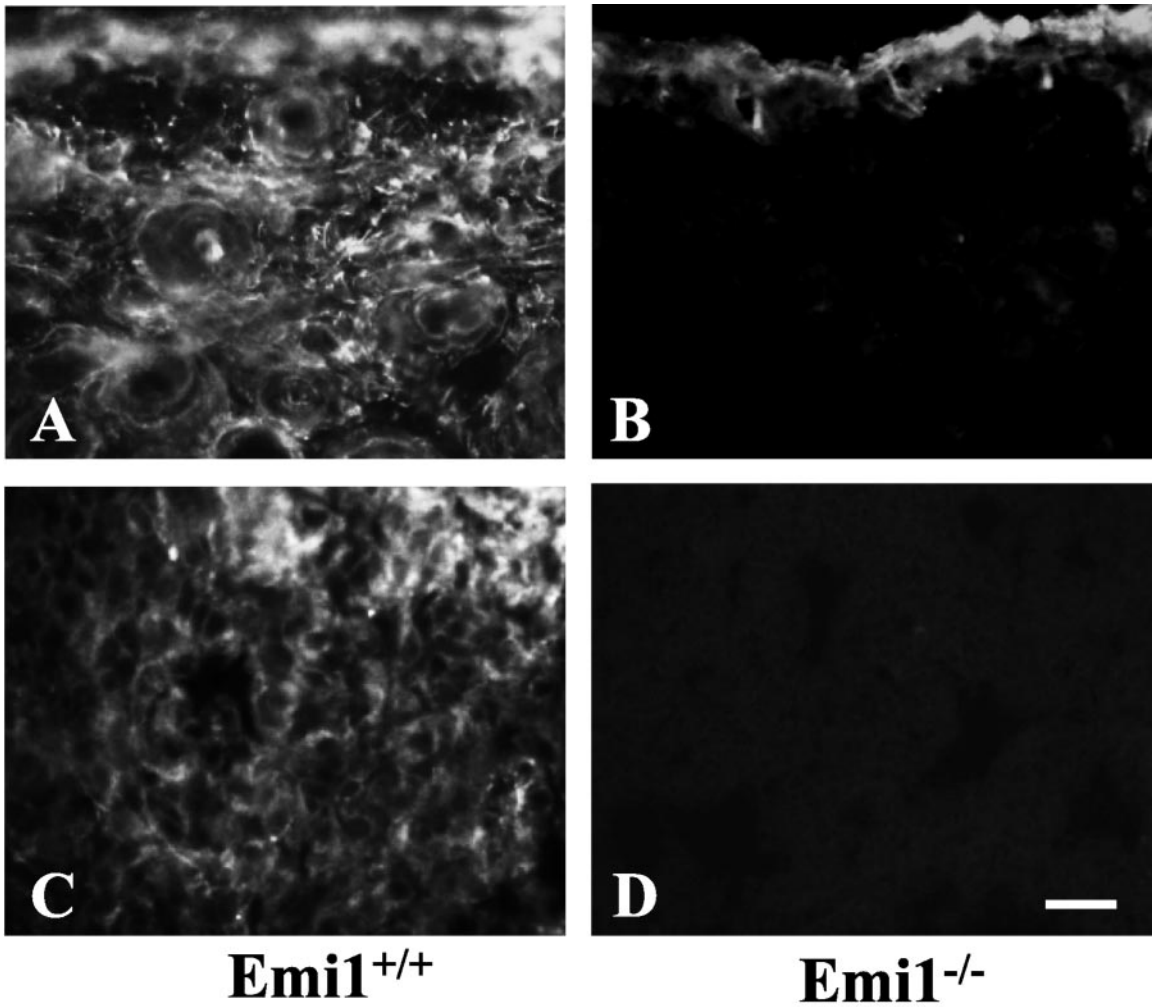

FIG. 2. EMILIN-1 is not deposited in the extracellular matrix of Emi1$^{-/-}$ mice. Cryostat sections of skin (A and B) and lung (C and D) from control (Emi1$^{+/+}$) (A and C) and EMILIN-1-deficient (Emi1$^{-/-}$) (B and D) mice were stained by immunofluorescence with a rat antibody against mouse EMILIN-1. The fluorescent layer present in skin sections is due to autofluorescence of the epidermis. Bar, 30 μm.

from EMILIN-1 deficient mice (Fig. 5E). As these alterations are reminiscent of cells undergoing apoptosis, the terminal deoxynucleotidyltransferase-mediated dUTP-biotin nick end labeling reaction was carried out on aorta sections. The numbers of apoptotic cells, which were extremely low, were not significantly different in control and mutant aortas (data not shown).

The elastic fiber alterations seen in aorta prompted us to search for gross vascular lesions in EMILIN-1-deficient mice. To this purpose, the main arteries, including the entire aorta and the initial tract of major vessels originating from it, were examined in several mutant mice at various ages. No obvious alterations (such as the presence of restriction sites or vessel lengthening) could be detected.

As these data imply a role for EMILIN-1 in elastogenesis, a series of experiments were performed to gain insight into the mechanism of EMILIN-1 regulation of elastic fiber formation. In one type of experiments, embryonic fibroblasts derived from control and EMILIN-1-deficient mice were grown in culture for several days and then stained by immunofluorescence with antibodies against elastic fiber components. Elastin staining of control fibroblasts showed that elastic fibers were mainly arcuate and frequently fused, giving rise to larger fibers (Fig. 6A). In mutant fibroblasts, fibers were usually straight and were fused less frequently (Fig. 6B). We next investigated whether deposition of different molecules into elastic fibers was affected by EMILIN-1 deficiency. Fibroblasts cultures were double stained with antibodies against elastin and other elastic fiber components, including fibrillin-1, the major constituent of microfibrils, and two proteins, fibulin-2 and fibulin-5, that, like EMILIN-1, associate with the amorphous core (29, 31, 34). Fibulin-5 was of particular interest in this context, as inactivation of its gene induces alterations of elastic fibers in different organs (29, 34). Fibrillin-1 colocalized with elastin in control fibroblasts, and the reciprocal pattern of distribution of the two proteins was not modified by EMILIN-1 deficiency (data not shown). Similar results were obtained for fibulin-2 (data not shown). In contrast, alterations of fibulin-5 deposition were detected in EMILIN-1 mutant compared with control fibroblasts (Fig. 7). As a general feature, fibulin-5 and elastin lo-

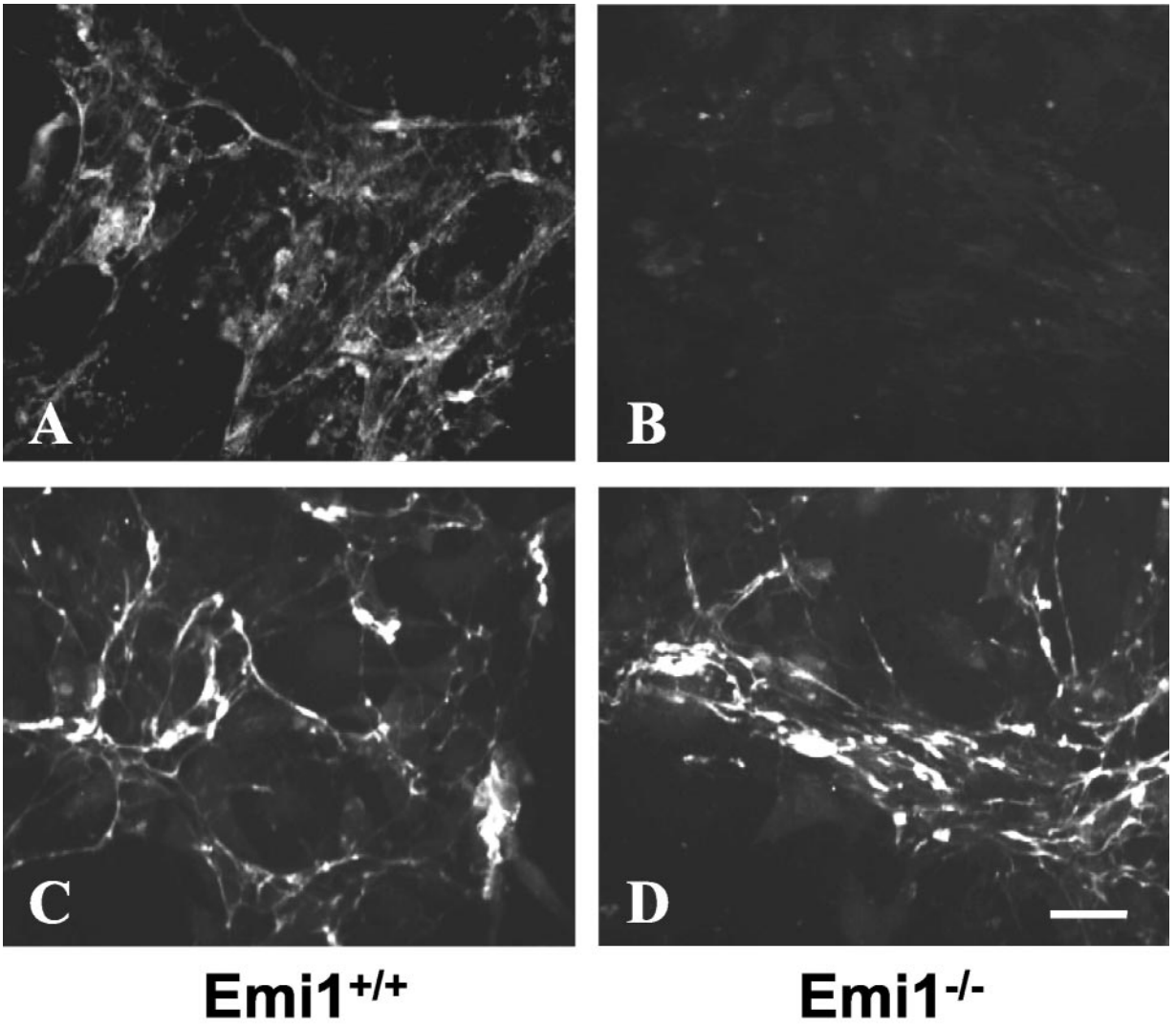

FIG. 3. Absence of EMILIN-1 does not alter the deposition of fibronectin in the extracellular matrix. Emi1$^{+/+}$ (A and C) or Emi1$^{-/-}$ (B and D) embryonic fibroblasts were stained by immunofluorescence with antibodies against EMILIN-1 (A and B) or fibronectin (C and D). Bar, 25 μm.

calizations overlapped in controls. This is clearly noticeable in Fig. 7C, a merge picture, where the color of fibers varies from green-yellow to orange depending on the relative abundance of fibulin-5 (stained green) to elastin (stained red) and in which each fiber is well defined and can be recognized in both the red and green channels (Fig. 7A and B). In EMILIN-1 mutant fibroblasts, while elastin distribution was markedly fibrillar and evenly spread in the culture layer (Fig. 7D), the pattern of fibulin-5 labeling was consistently altered (Fig. 7E and F). Staining was mostly concentrated at large elastin deposits, whereas it faded rapidly in fibrils irradiating from them. Moreover, the design of fibrillar structures appeared less defined and blurred, and a number of elastin deposits were not matched by fibulin-5 staining (Fig. 7D to F).

The results just described suggest interactions of EMILIN-1 with some components of elastic fibers, most likely elastin and fibulin-5. Therefore, a second series of experiments, aimed at identifying proteins that bind EMILIN-1, was performed. Solid-phase interaction assays showed that EMILIN-1 binds strongly to human α-elastin (Fig. 8A) and to chicken α-elastin (data not shown) but not to a host of proteins of the extracellular matrix included as control (Fig. 8A). Both EMILIN-1 aggregates and the monomeric form of EMILIN-1, a homotrimer of identical polypeptide chains, were effective in binding elastin, while the interaction was largely lost when EMILIN-1 was heat denatured (Fig. 8A).

This interaction was confirmed by immunoprecipitation assays with proteins produced by 293T cells transfected with mixtures of cDNA constructs coding for elastin and EMILIN-1. A band with the mobility of EMILIN-1 was detected in both the culture medium and cell extract after immunoprecipitation with anti-α-elastin antibodies and subsequent Western blotting with anti EMILIN-1 antibodies (Fig. 8B, left panel). A similar band was identified when cells were cotransfected with fibulin-5 and EMILIN-1 cDNAs and the proteins immunoprecipitated with anti-fibulin-5 antibody were analyzed by immunoblotting with the antiserum to EMILIN-1 (Fig. 8B, right

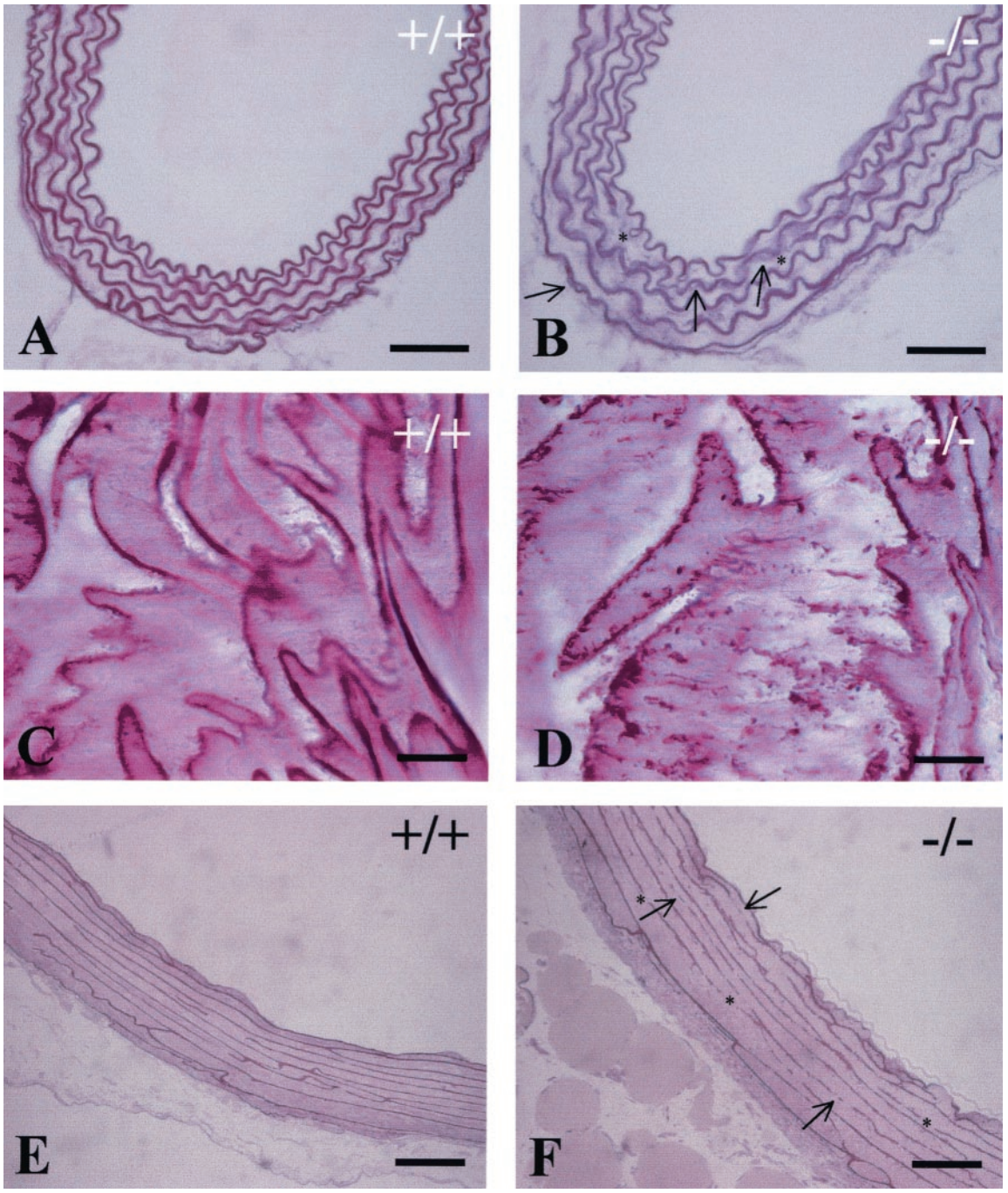

FIG. 4. Histological alterations of aorta in EMILIN-1-deficient mice. (A, C, and E) Control animals; (B, D, and F) knockout animals. Sections were cut from paraffin-embedded (A to D) or Epon-embedded (E and F) adult ascending aorta and stained with Weigert solution. (A and B) Elastic laminae from mutant animals have an irregular outline, are more frequently interrupted (asterisks), and are often delaminated (arrows). (C and D) In addition to the rough surface of elastic laminae, oblique sections show irregular elastin deposits between the laminae. (E and F) Regions of fragmentation of elastic laminae can be seen in semithin sections. Bars. 50 μm (A, B, E, and F) and 20 μm (C and D).

panel). This result suggests a direct interaction of EMILIN-1 with fibulin-5.

Additional experiments were performed to establish whether production and processing of the soluble elastin precursor tropoelastin in vivo was altered by the absence of EMILIN-1. To this purpose, aortas from normal and mutant mice were extracted in the presence of 8 M urea. Aliquots of the extracts were resolved by SDS-PAGE, and migration of elastin peptides was identified by Western blotting (Fig. 9). The pattern of bands that appeared in both extracts was complex, including a band with the mobility expected for tropoelastin and higher-molecular-weight species. The striking difference

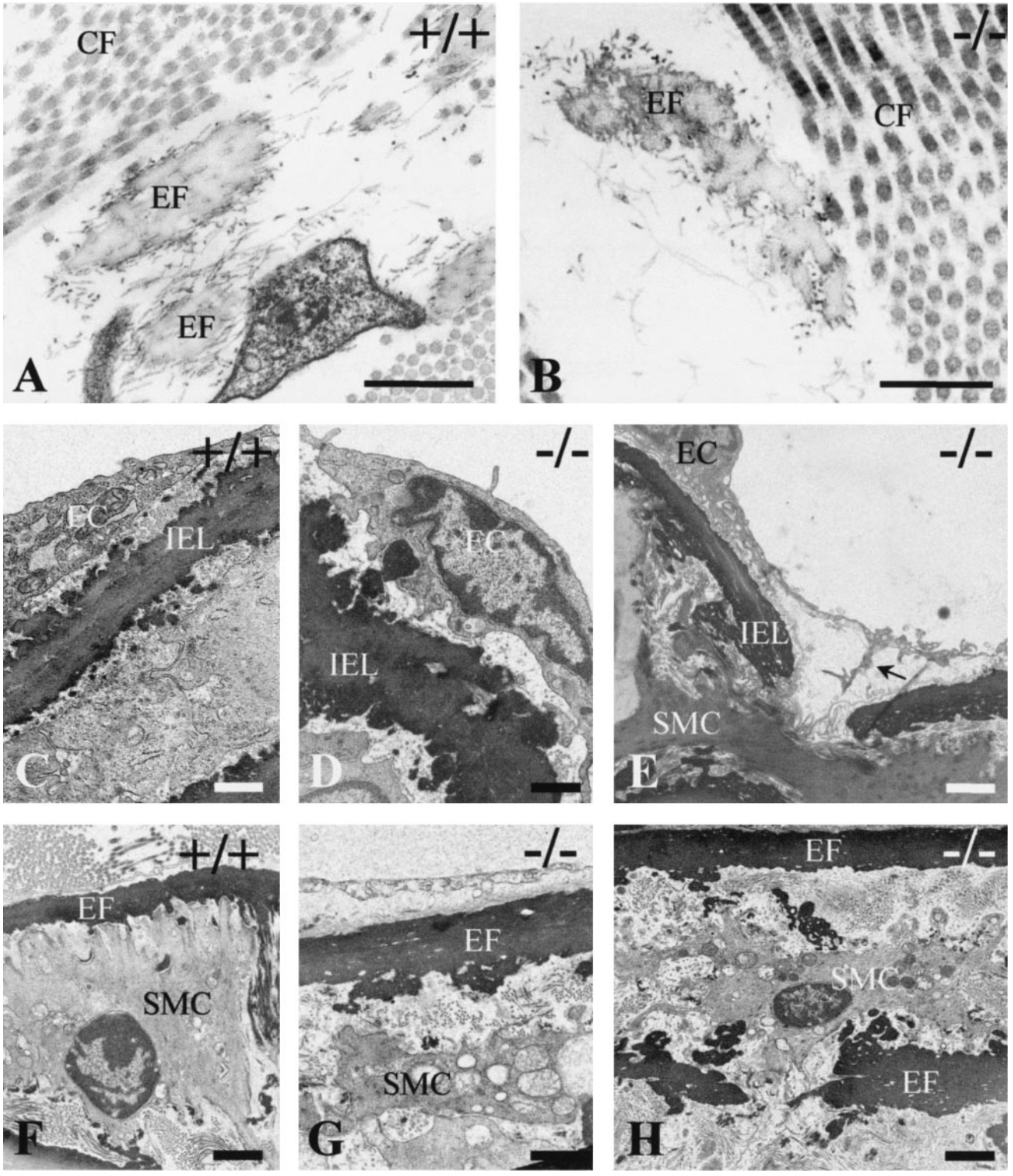

FIG. 5. Ultrastructural defects in EMILIN-1 deficient mice. (A and B) Electron micrographs showing elastic fibers from skin of normal (A) and knockout (B) mice. Normal fibers are compact and have an even outline, while frequent indentations give mutant fibers an irregular appearance. (C to E) Endothelial cells and internal elastic laminae from normal (C) and mutant (D and E) animals. The electron micrographs show an enlarged space between the cell and the elastic lamina in EMILIN-1-deficient mice (compare panels C and D). Alteration of an endothelial cell at sites of interruption of the internal elastic lamina is seen in panel E. The arrow indicates endothelial cell protrusion into the enlarged space between the cell and the internal elastic lamina. (F to H) Abnormalities of smooth muscle cell morphology. The normal anchorage of smooth muscle cells to elastic laminae (F) is often lost in knockout animals (G and H), and cells exhibit enlarged organelles and condensed chromatin. CF, collagen fibers; EC, endothelial cell; EF, elastic fiber; IEL, internal elastic lamina; SMC, smooth muscle cell. Bars, 0.5 μm (A, B, C, D, F, G, and H) and 1.5 μm (E).

TABLE 2. Quantitative analysis of abnormal cells in aortas

Cells	Mice	% of cells with morphological alterations[a] (Avg ± SD)	*P* value (Student's *t* test)
Endothelial	Emi1$^{-/-}$	47 ± 9	<0.00001
	Emi1$^{+/+}$	13 ± 2	
Smooth muscle	Emi1$^{-/-}$	20 ± 5	<0.00001
	Emi1$^{+/+}$	3 ± 1	

[a] Alterations considered are those described in the text and exemplified in Fig. 5. Numbers were calculated by using cell counts from six Emi1$^{-/-}$ and four Emi1$^{+/+}$ 2-month-old mice. The total numbers of smooth muscle cells counted were 2,182 (Emi1$^{-/-}$ aortas) and 1,400 (Emi1$^{+/+}$ aortas). The corresponding numbers for endothelial cells were 161 (Emi1$^{-/-}$ aortas) and 91 (Emi1$^{+/+}$ aortas). Aortas from one Emi1$^{-/-}$ mouse and one Emi1$^{+/+}$ mouse were dissected after perfusion of the animals with 2.5% glutaraldehyde in PBS. The data obtained from these samples were indistinguishable from those derived from aortas fixed by immersion into 2.5% glutaraldehyde immediately after dissection.

between the control and knockout samples was the presence of a doublet of reactive bands of about 50 kDa only in mutant aorta. These bands may well represent degradation products of tropoelastin (or elastin). These data suggest that in the absence of EMILIN-1, degradation of tropoelastin (or elastin) is increased.

Finally, the possibility that the expression of other genes of elastic fibers was affected in EMILIN-1 mutant mice was tested. No variations of mRNAs for elastin and fibrillin-1, the two major components of elastic fibers, were detected by Northern blot analysis during development, at birth, and in adult tissues (data not shown); also, a lack of EMILIN-1 did not alter expression of mRNAs of the other members of the EMILIN family (data not shown).

DISCUSSION

The results reported in this paper imply a function for EMILIN-1 in elastogenesis and maintenance of vascular cell morphology. A role of the protein in elastic fiber formation was previously suggested in studies in vitro, where the process was disrupted by the addition of anti-EMILIN antibodies (5). In vivo, the absence of EMILIN-1 affects the amorphous core of elastic fibers, which appears irregularly shaped and split, whereas the microfibrillar coat is normal. This is consistent with the preferred ultrastructural location of EMILIN-1 at the surface of the amorphous core and not on microfibrils (5). In vitro, analyses of mutant embryonic fibroblasts show a reduced tendency of elastin deposits to coalesce into larger fibers, thus giving rise to the formation of thin and straight fibers. All of these alterations, both in vivo and in vitro, can be explained by assuming that the role of EMILIN-1 in elastogenesis is to favor the fusion of elastin deposits in a way that renders them more homogeneous and even.

The finding that EMILIN-1 binds specifically to elastin suggests one possible mechanism of EMILIN-1 function in elastogenesis. EMILIN-1 is present mainly as disulfide-bonded high-molecular-weight aggregates in the extracellular matrix (4, 8, 27); it is therefore possible that such complexes bridge many different elastin precursor molecules or fibrous elastin deposits, thus promoting merging of newly synthesized fibers. A second mechanism, which is not alternative but may be simultaneous, is implied by the observation of polypeptide species with molecular weights lower of that of tropoelastin only in aortas of mutant mice, a result suggesting the intriguing possibility that EMILIN-1 protects, in an unknown way, tropoelastin (or elastin) from degradation. In this alternative, the lack of EMILIN-1 would increase the presence of tropoelastin-soluble species that may be incorporated less efficiently into

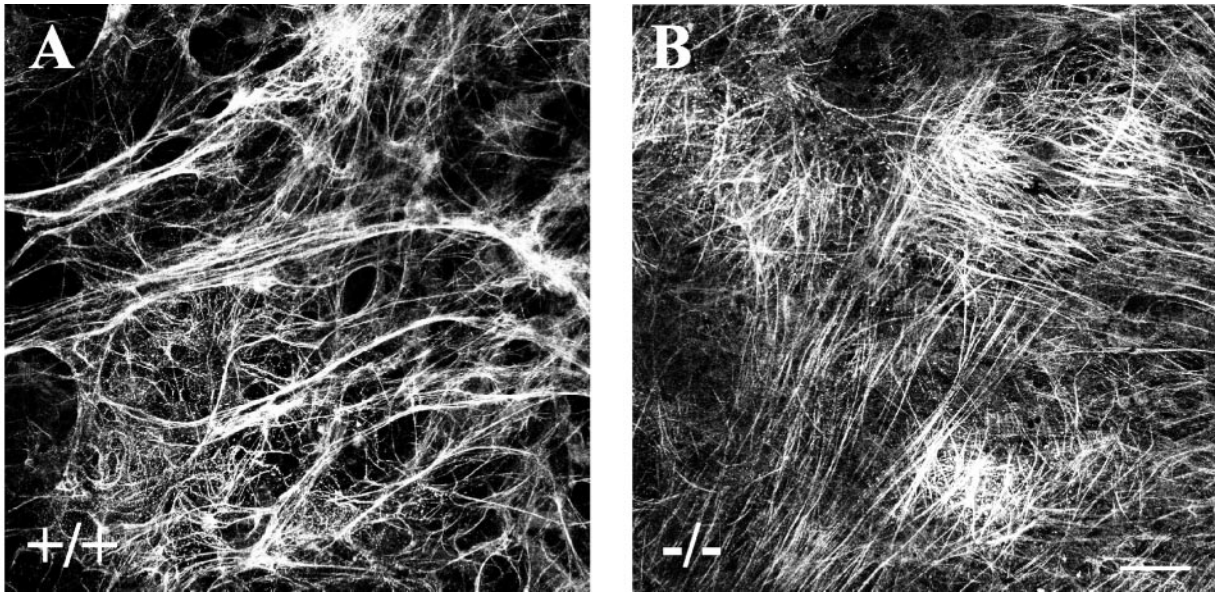

FIG. 6. Elastogenesis in mouse embryo fibroblast cultures. Mouse embryo fibroblasts from control (A) and mutant (B) animals were cultured for 15 days, stained with antibodies against mouse elastin, and observed in a confocal microscope. Note the decreased tendency to fusion and the straighter organization of fibers in knockout animals. Bar, 20 μm.

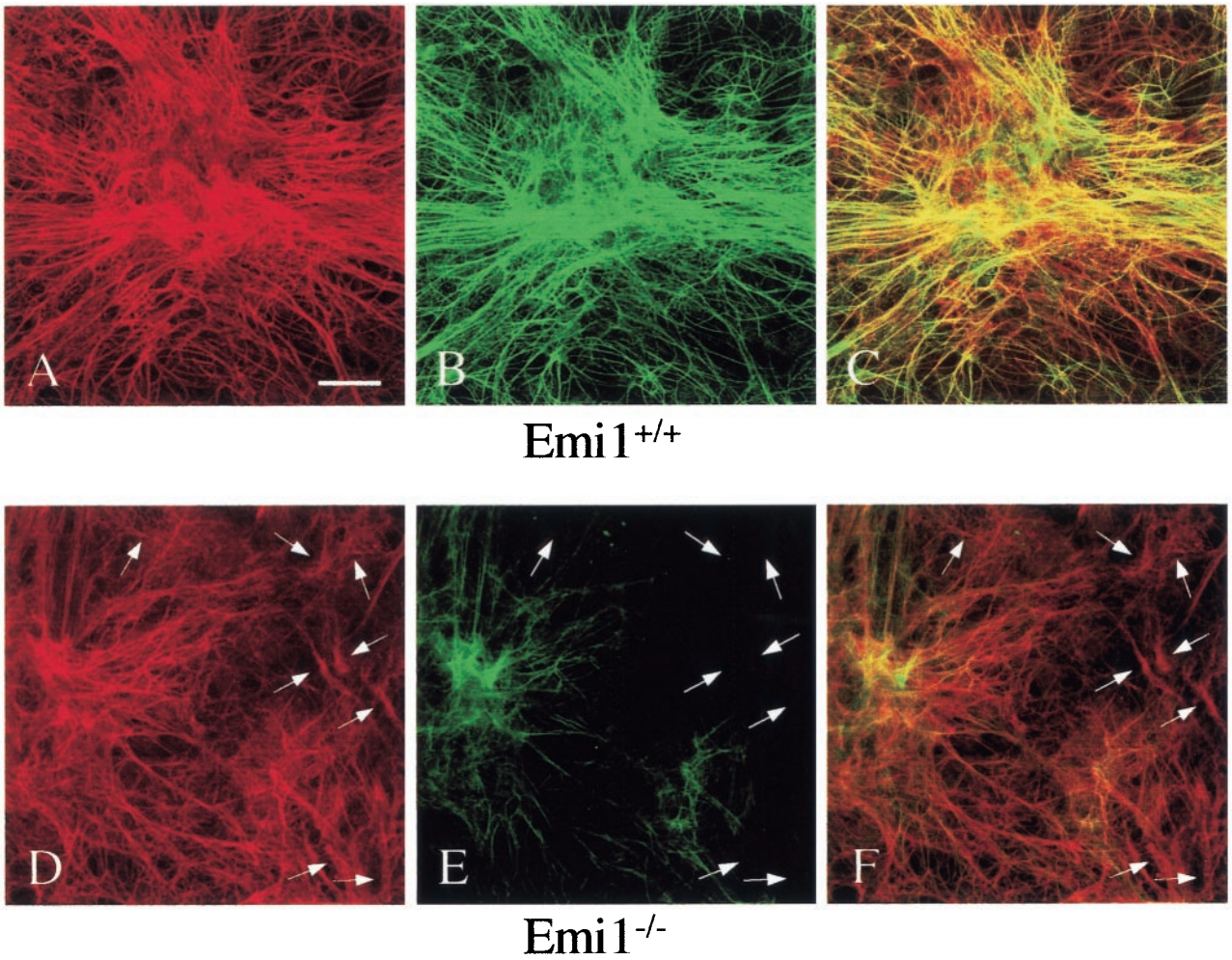

FIG. 7. Alteration of fibulin-5 deposition pattern in EMILIN-1-deficient fibroblasts. Embryonic mouse embryo fibroblasts from control (A to C) and mutant (D to F) mice were grown in chamber slides for 10 days, and the distributions of elastin (A and D) and fibulin-5 (B and E) incorporated into the extracellular matrix were visualized by double immunostaining and observation in the confocal microscope. In panels C and F, the fluorescent stainings for the two proteins were merged. In EMILIN-1 mutant cells fibulin-5 staining was found mostly on large elastin condensations, whereas it appeared less defined than in controls and rapidly fading on thinner fibers radiating from the larger deposits. Moreover, the strict correspondence of elastin and fibulin-5 staining seen in control samples was often lost, with the consequent appearance of elastin deposits (arrows in panel D) and with no staining for fibulin-5 at the corresponding sites (arrows in panels E and F). Bar, 30 μm.

fibrous deposits or hamper the deposition of elastic fibers with a regular morphology. A third mechanism, also not alternative to those just mentioned, may be related to the interaction of EMILIN-1 with fibulin-5. Similarly to EMILIN-1, this protein is localized at the amorphous elastin-microfibril interface and is adhesive for cells (29, 34). The targeted inactivation of fibulin-5 induces ultrastructural alterations of elastic fibers similar to, although more severe than, those observed in EMILIN-1-deficient mice and a phenotype of elastic fiber failure (29, 34). Thus, the absence of EMILIN-1 may produce elastic fiber abnormalities by partially destabilizing the function of fibulin-5.

An important defect observed in EMILIN-1-deficient mice relates to the connection of vascular cells to elastic lamellae. In EMILIN-1-deficient mice, some cells appear to have lost their connections with the elastic lamellae, from which they are separated by an enlarged space filled with loose extracellular matrix. What determines this condition is presently unknown. Immunoelectron microscopy has revealed that filaments connecting endothelial cells to the internal elastic lamella associate with different extracellular matrix proteins, including fibrillin-1, fibronectin, and heparan sulfate proteoglycan (13). In the aortic media, extensions of elastic lamellae attach to the cell surface and microfibrils can be morphologically identified at the sites of contact, which are characterized by the presence of cytoplasmic densities (14). One possibility is that EMILIN-1 is a component of the system of anchorage of cells to elastic lamellae; the absence of the protein would weaken these connections, and cells would detach from the lamellae and round up. Alternatively, cellular alterations may be the consequence of defective elastic fibers; instead of resisting stress, as under normal conditions, elastic fibers would be disrupted by cellular contraction, and the absence of a sub-

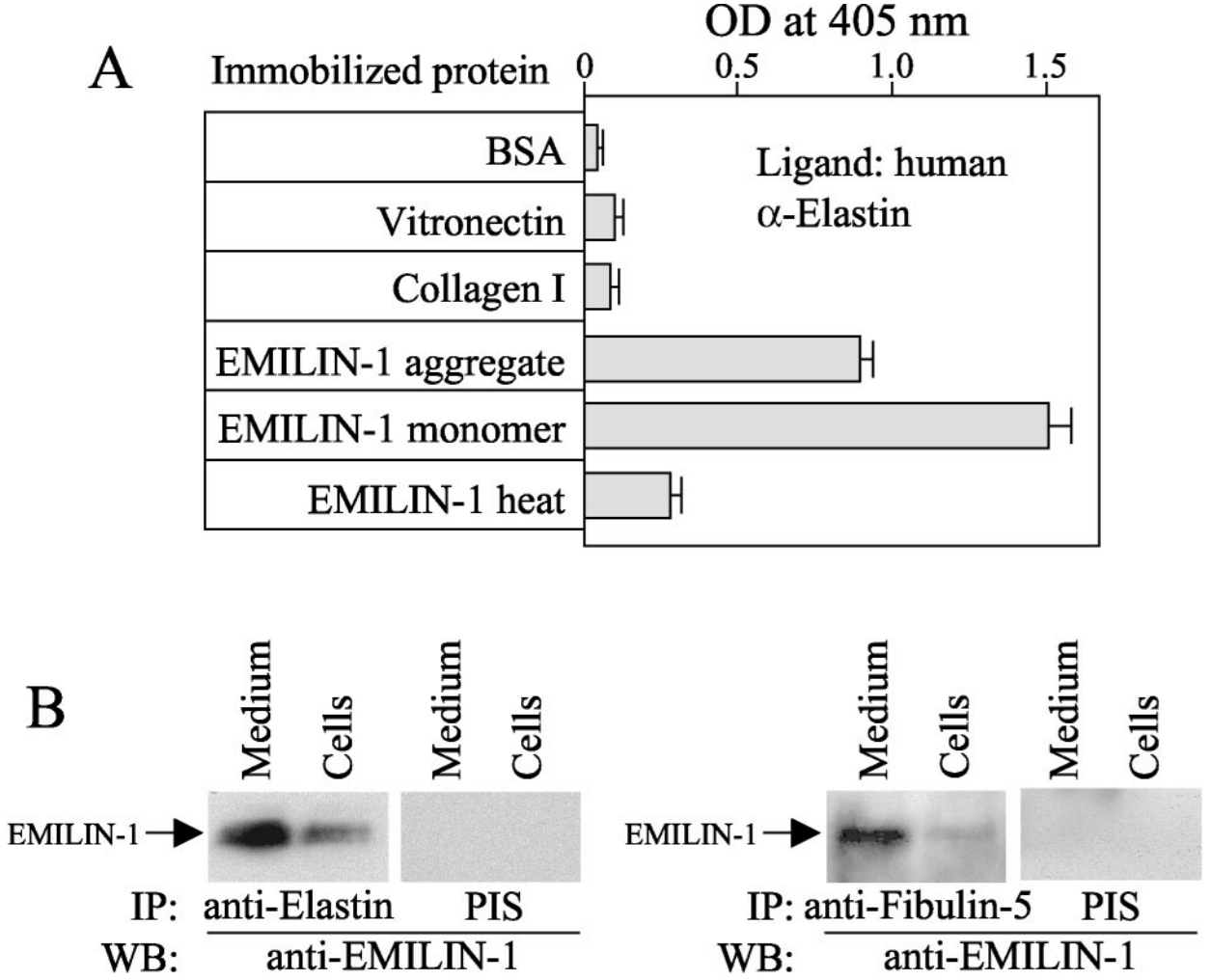

FIG. 8. Molecular interactions of EMILIN-1. (A) Solid-phase binding assay disclosing specific interaction of EMILIN-1 with elastin. Concentrations of 0.5 μg of different proteins per well immobilized on 96-well plates were reacted with soluble human α-elastin, and the interaction was revealed with an antibody to human α-elastin (1:2,000 dilution) followed by HRP-labeled secondary antibody and a color reaction. Intensities similar to those reported for type I collagen and vitronectin were also observed with fibronectin, Engelbreth-Holm-Swarm laminin-1, a mixture of laminin-1/10/11, and type VI collagen (data not shown). Specific binding was also detected when elastin was immobilized on plates and EMILIN-1 was employed as a soluble ligand or when chicken instead of human α-elastin was used (data not shown). OD, optical density. (B) Immunoprecipitation assays showing binding of EMILIN-1 to elastin and fibulin-5. 293T cells were transfected with a mixture of elastin and EMILIN-1 (left panel) or of fibulin-5 and EMILIN-1 (right panel) expression plasmids, and the culture medium and the cell layer extract were processed for immunoprecipitation (IP) with antibodies to α-elastin (left panel) or fibulin-5 (right panel). The immunoprecipitates were then analyzed by Western blotting (WB) with anti-EMILIN-1 antibodies. Control samples were immunoprecipitated with preimmune serum (PIS) and similarly processed.

strate resisting tension would determine a morphology similar to that of cells in suspension.

An additional finding in EMILIN-1-deficient aorta was the presence of cells with clear morphological alterations consisting of an enlarged endoplasmic reticulum, swollen or dense mitochondria, and nuclei with condensed or pycnotic chromatin. The number of these altered cells, both endothelial and smooth muscle, differed in a highly significant way in mutant and normal animals. The mechanism inducing these alterations is unknown. As contact with the extracellular matrix is considered to be important for maintenance of cell morphology and survival, the adhesive function of EMILIN-1 (18, 32) may well be involved. EMILIN-1 interacts with the cell surface through its gC1q-like domain, and the cell receptor identified so far is integrin α4-β1. This integrin is expressed mainly in leukocytes in the adult, and known ligands include VCAM-1, fibronectin, and osteopontin (26). Expression has also been detected in vascular cells during development but not in normal adult cells. Interestingly, however, production of α4 integrin can be resumed after cell activation in pathological conditions, such as atherosclerosis. The implication of α4-β1 integrin as a receptor of EMILIN-1 for the maintenance of vascular smooth muscle and endothelial cell homeostasis is at the moment an attractive hypothesis for future work on the characterization of EMILIN-1-deficient mice. Overall, the morphological findings are indicative of altered cellular homeostasis. Although apoptosis was not detected, this condition may compromise cellular adaptation to vascular stress, such as hypertension and atherogenic stimuli.

In summary, our data demonstrate that EMILIN-1 has a

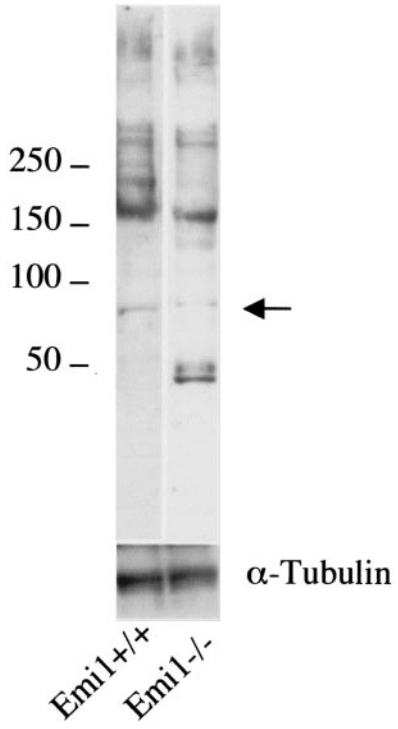

FIG. 9. Tropoelastin-related peptides in aorta extracts from control (Emi1$^{+/+}$) and EMILIN-1 mutant (Emi1$^{-/-}$) mice. Proteins extracted in the presence of 8 M urea were analyzed by SDS-PAGE and Western blotting with antielastin antibodies. Numbers indicate the migration of protein standards with the defined molecular weights. The arrow marks a reactive band with the mobility expected for tropoelastin. As a loading control, the filters were reacted with antibodies to α-tubulin.

role in elastogenesis and maintenance of vascular cell morphology. Considering that EMILIN-1 is one of a family of four genes with similar structural organizations and similar expression patterns (24), the mildness of the phenotypic alterations consequent to its deficiency may be due to genetic compensation by other EMILINs. At present no human hereditary disease involving EMILINs is known. The morphological abnormalities revealed in this study constitute the first potential hallmark of EMILIN-1 insufficiency and may be helpful for the identification of heritable diseases induced by mutations of this gene.

ACKNOWLEDGMENTS

This work was supported by Telethon grant E.704, by a PRIN-2000 grant from the Italian MIUR, and by Progetto Strategico MURST "Genetica Molecolare" (grant 01.00858.ST9).

We thank R. Mecham for the antibodies against mouse tropoelastin, R. Timpl for antibodies to fibulin-2, and H. Yanagisawa for fibulin-5 antiserum and the cDNA clone. We also thank Tania Tiepolo for technical help.

REFERENCES

1. **Ausubel, F. M., R. Brent, R. E. Kingston, D. D. Moore, J. A. Smith, J. S. Seidman, and K. Struhl.** 1993. Current protocols in molecular biology. John Wiley & Sons, Inc., New York, N.Y.
2. **Bonaldo, P., P. Braghetta, M. Zanetti, S. Piccolo, D. Volpin, and G. M. Bressan.** 1998. Collagen VI deficiency induces early onset myopathy in the mouse: an animal model for Bethlem myopathy. Hum. Mol. Genet. **7:**2135–2140.
3. **Braghetta, P., A. Ferrari, P. de Gemmis, M. Zanetti, D. Volpin, P. Bonaldo, and G. M. Bressan.** 2002. Expression of the EMILIN-1 gene during mouse development. Matrix Biol. **21:**603–609.
4. **Bressan, G. M., I. Castellani, A. Colombatti, and D. Volpin.** 1983. Isolation and characterization of a 115,000-dalton matrix-associated glycoprotein from chick aorta. J. Biol. Chem. **258:**13262–13267.
5. **Bressan, G. M., D. Daga-Gordini, A. Colombatti, I. Castellani, V. Marigo, and D. Volpin.** 1993. Emilin, a component of elastic fibers preferentially located at the elastin-microfibrils interface. J. Cell Biol. **121:**201–212.
6. **Christian, S., H. Ahorn, M. Novatchkova, P. Garin-Chesa, J. E. Park, G. Weber, F. Eisenhaber, W. J. Rettig, and M. C. Lenter.** 2001. Molecular cloning and characterization of EndoGlyx-1, an EMILIN-like multisubunit glycoprotein of vascular endothelium. J. Biol. Chem. **276:**48588–48595.
7. **Colombatti, A., K. Ainger, and F. Colizzi.** 1989. Type VI collagen: high yields of a molecule with multiple forms of alpha 3 chain from avian and human tissues. Matrix **9:**177–185.
8. **Colombatti, A., P. Bonaldo, D. Volpin, and G. M. Bressan.** 1988. The elastin associated glycoprotein gp115. Synthesis and secretion by chick cells in culture. J. Biol. Chem. **263:**17534–17540.
9. **Colombatti, A., G. M. Bressan, I. Castellani, and D. Volpin.** 1985. Glycoprotein 115, a glycoprotein isolated from chick blood vessels, is widely distributed in connective tissue. J. Cell Biol. **100:**18–26.
10. **Colombatti, A., R. Doliana, S. Bot, A. Canton, M. Mongiat, G. Mungiguerra, S. Paron-Cilli, and P. Spessotto.** 2000. The EMILIN protein family. Matrix Biol. **19:**289–301.
11. **Colombatti, A., A. Poletti, G. M. Bressan, A. Carbone, and D. Volpin.** 1987. Widespread codistribution of glycoprotein gp 115 and elastin in chick eye and other tissues. Coll. Relat. Res. **7:**259–275.
12. **Daga-Gordini, D., G. M. Bressan, I. Castellani, and D. Volpin.** 1987. Fine mapping of tropoelastin-derived components in the aorta of developing chick embryo. Histochem. J. **19:**623–632.
13. **Davis, E. C.** 1993. Endothelial cell connecting filaments anchor endothelial cells to the subjacent elastic lamina in the developing aortic intima of the mouse. Cell Tissue Res. **272:**211–219.
14. **Davis, E. C.** 1993. Smooth muscle cell to elastic lamina connections in developing mouse aorta. Role in aortic medial organization. Lab. Invest. **68:**89–99.
15. **Doliana, R., S. Bot, P. Bonaldo, and A. Colombatti.** 2000. EMI, a novel cysteine-rich domain of EMILINs and other extracellular proteins, interacts with the gC1q domains and participates in multimerization. FEBS Lett. **484:**164–168.
16. **Doliana, R., S. Bot, G. Mungiguerra, A. Canton, S. P. Cilli, and A. Colombatti.** 2001. Isolation and characterization of EMILIN-2, a new component of the growing EMILINs family and a member of the EMI domain-containing superfamily. J. Biol. Chem. **276:**12003–12011.
17. **Doliana, R., A. Canton, F. Bucciotti, M. Mongiat, P. Bonaldo, and A. Colombatti.** 2000. Structure, chromosomal localization, and promoter analysis of the human elastin microfibril interface located proteIN (EMILIN) gene. J. Biol. Chem. **275:**785–792.
18. **Doliana, R., M. Mongiat, F. Bucciotti, E. Giacomello, R. Deutzmann, D. Volpin, G. M. Bressan, and A. Colombatti.** 1999. EMILIN, a component of the elastic fiber and a new member of the C1q/tumor necrosis factor superfamily of proteins. J. Biol. Chem. **274:**16773–16781.
19. **Hayward, C. P., J. A. Hassell, G. A. Denomme, R. A. Rachubinski, C. Brown, and J. G. Kelton.** 1995. The cDNA sequence of human endothelial cell multimerin. A unique protein with RGDS, coiled-coil, and epidermal growth factor-like domains and a carboxyl terminus similar to the globular domain of complement C1q and collagens type VIII and X. J. Biol. Chem. **270:**18246–18251.
20. **Hogan, B., F. Costantini, and E. Lacey.** 1994. Manipulating the mouse embryo. A laboratory manual. Cold Spring Harbor Laboratory Press, Cold Spring Harbor, N.Y.
21. **Kaestner, K. H., L. Montoliu, H. Kern, M. Thulke, and G. Schutz.** 1994. Universal beta-galactosidase cloning vectors for promoter analysis and gene targeting. Gene **148:**67–70.
22. **Kohfeldt, E., P. Maurer, C. Vannahme, and R. Timpl.** 1997. Properties of the extracellular calcium binding module of the proteoglycan testican. FEBS Lett. **414:**557–561.
23. **Laird, P. W., A. Zijderveld, K. Linders, M. A. Rudnicki, R. Jaenisch, and A. Berns.** 1991. Simplified mammalian DNA isolation procedure. Nucleic Acids Res. **19:**4293.
24. **Leimeister, C., C. Steidl, N. Schumacher, S. Erhard, and M. Gessler.** 2002. Developmental expression and biochemical characterization of Emu family members. Dev. Biol. **249:**204–218.
25. **Lindblom, A., T. Marsh, C. Fauser, J. Engel, and M. Paulsson.** 1994. Characterization of native laminin from bovine kidney and comparison with other laminin variants. Eur. J. Biochem. **219:**383–392.
26. **Liu, S., D. M. Rose, J. Han, and M. H. Ginsberg.** 2000. Alpha4 integrins in cardiovascular development and diseases. Trends Cardiovasc. Med. **10:**253–257.
27. **Mongiat, M., G. Mungiguerra, S. Bot, M. T. Mucignat, E. Giacomello, R.**

Doliana, and A. Colombatti. 2000. Self-assembly and supramolecular organization of EMILIN. J. Biol. Chem. **275:**25471–25480.
28. **Nagy, A., J. Rossant, R. Nagy, W. Abramow-Newerly, and J. C. Roder.** 1993. Derivation of completely cell culture-derived mice from early-passage embryonic stem cells. Proc. Natl. Acad. Sci. USA **90:**8424–8428.
29. **Nakamura, T., P. R. Lozano, Y. Ikeda, Y. Iwanaga, A. Hinek, S. Minamisawa, C. F. Cheng, K. Kobuke, N. Dalton, Y. Takada, K. Tashiro, J. Ross, Jr., T. Honjo, and K. R. Chien.** 2002. Fibulin-5/DANCE is essential for elastogenesis in vivo. Nature **415:**171–175.
30. **Partridge, S. M., H. F. Davis, and G. S. Adair.** 1955. Soluble proteins derived from partial hydrolysis of elastin. Biochem. J. **61:**11–21.
31. **Sasaki, T., W. Gohring, N. Miosge, W. R. Abrams, J. Rosenbloom, and R. Timpl.** 1999. Tropoelastin binding to fibulins, nidogen-2 and other extracellular matrix proteins. FEBS Lett. **460:**280–284.
32. **Spessotto, P., M. Cervi, M. T. Mucignat, G. Mungiguerra, I. Sartoretto, R. Doliana, and A. Colombattti.** 2003. Beta 1 integrin-dependent cell adhesion to EMILIN-1 is mediated by the gC1q domain. J. Biol. Chem. **278:**6170–6177.
33. **Tso, J. Y., X. H. Sun, T. H. Kao, K. S. Reece, and R. Wu.** 1985. Isolation and characterization of rat and human glyceraldehyde-3-phosphate dehydrogenase cDNAs: genomic complexity and molecular evolution of the gene. Nucleic Acids Res. **13:**2485–2502.
34. **Yanagisawa, H., E. C. Davis, B. C. Starcher, T. Ouchi, M. Yanagisawa, J. A. Richardson, and E. N. Olson.** 2002. Fibulin-5 is an elastin-binding protein essential for elastic fibre development in vivo. Nature **415:**168–171.
35. **Yatohgo, T., M. Izumi, H. Kashiwagi, and M. Hayashi.** 1988. Novel purification of vitronectin from human plasma by heparin affinity chromatography. Cell Struct. Funct. **13:**281–292.